Noise characterisation of multi-propeller under static conditions in hover

Mansi Bhardwaj*, Philip Woodhead†, Max Scholz‡, and Tze Pei Chong§
Brunel University London, Uxbridge, UB8 3PH, UK

This paper represents an experimental study on the aeroacoustics behaviours of multi-propellers. Two propellers are distributed in various spatial configurations to mimic some of the configurations that resemble a typical eVTOL (electrical Vertical Take-Off and Landing) aircraft. The interdependence for various influencing parameters for the acoustic radiations, such as the longitudinal and transverse displacements between a reference propeller and another propeller, as well as the different rotational speeds, was investigated in a specially constructed test rig inside an anechoic chamber under a quiescent condition. Statistical quantities such as the power spectral density and overall sound pressure level are presented.

I. Introduction

The emerging notion of eVTOL commonly referred to as Air-taxis is becoming popular because of the fascinating impact it will have on our lifestyles like on-demand passenger and cargo transportation, fast emergency responses, better reach to remote locations etc. while making transportation faster and cheaper. This popularity is visible by an advent increase in the growth of the eVTOL market, which also raises the concerns related to the noise generated by these vehicles [1]. Vertical Take-Off and Landing vehicles use rotors to produce enough thrust to lift and move the vehicle. In general, eVTOL vehicles use smaller multiple propellers to generate thrust.

Noise generated by these multiple propellers is very severe and loud, thereby limiting a fast and widespread adoption of eVTOLs. Many researches are dedicated to understand the noise of single propellers under variable conditions [2–4], and various multi-rotor configurations that encompass a wide range of transverse (side-by-side) separation distances between the propellers [5–8], as well as in tandem configurations [9]. Zhou *et al.* [5] show that the periodic vortex shedding and rotor to rotor interactions are very dominant for the twin rotor cases compared to the single rotor case, which could lead to higher thrust fluctuations. These thrust fluctuations were also noticed by Bu *et al.* [7] in their study of two co-rotating propellers mounted side-by-side with a minimum separation gap.

Bu *et al.* [6] studies the effect of multi-propeller noise generation in a side-by-side configuration. They demonstrate that the noise generation is affected more significantly by the lateral tip spacing, and is relatively less sensitive to the axial separation distance. The radiated tonal noise level is observed to increase while observing from low angles. However, the broadband noise levels remain largely unaffected, which could be due to an underdeveloped wake in their study. When three propellers are present in a side-by-side configuration [8], the presence of adjacent propellers deteriorates the performance of the middle propeller. This configuration also increases the noise level by more than 9 dB while also adding numerous higher harmonics in the noise spectra.

When the propellers are in tandem configuration [9], the slipstream of the front propeller interrupts the flow over the rear propeller depending on the degree of overlaps. When the overlap between the propellers increase, there will be a noticeable reduction in the aerodynamic performance for the rear propeller. Rotors when placed in tandem configuration will induce complicated flow interactions, and result in the radiation of high noise level as compared to a single propeller configuration. The radiated noise level will also increase as the inflow velocity increases. When the forward propeller is at a tilt angle compared to the rear propeller, the overall noise level is reported to be lesser than in the case of no tilt [10]. Shukla *et al.* [11] performed PIV investigations on tandem configurations at low Reynolds number ranging from 40,000 to 80,000. They reported an interesting observation where the front rotor in a tandem design will perform better than the isolated propeller at low Reynolds numbers.

Propeller noise is also studied in a contra-rotating configuration. It is observed by Chaitanya *et al.* [12] that there exists an optimum separation distance for the best performance of propellers. Below this optimal range, the potential

*Doctoral Researcher, Department of Mechanical and Aerospace Engineering/mansi.bhardwaj@brunel.ac.uk,AIAA Student Member.
†Research Fellow, Department of Mechanical and Aerospace Engineering/philip.woodhead2@brunel.ac.uk, and AIAA Member.
‡Doctoral Researcher, Department of Mechanical and Aerospace Engineering/Max.Scholz@brunel.ac.uk,AIAA Student Member.
§Reader, Department of Mechanical and Aerospace Engineering/t.p.chong@brunel.ac.uk, AIAA Member.

field interactions dominate the overall noise radiation. On the other hand, above this optimal range one will see a dominant tip vortex interactions and the ensuing enhanced tip vortex noise radiation. They reported that the highest noise radiation occurs at a partial overlap of $d/D = 0.5$, where d is the separation distance and D is the diameter of propeller. The reason for which is believed to be the increased levels of flow non-symmetry and non-uniformity on the rear propeller.

The literature thus far confirms that the addition of extra propeller not only will increase the noise level, but also will create a complex interactive flow field. However, most of the studies focus on either the side-by-side, or tandem configurations only, albeit some with minor geometrical variations. From the perspective of the azimuthal angle, most of them only cover either 0° or 90°, respectively. They do not cover the entire range of location for the propellers at other azimuthal angles when the propellers are moved in space on a 2-dimensional plane (x-y, see figure 1) with respect to a stationary observer. This will create complex rotor-rotor wake interactions, and make the prediction of aeroacoustics performance difficult. This research gap motivates the present work, which uses a specially designed test rig to investigate the interdependence for various influencing parameters for the acoustic radiations, such as the longitudinal and transverse displacements between a reference propeller and another propeller, as well as the different rotational speeds.

II. Experimental Setup

A. Experimental facility

Experiments were performed in the anechoic chamber at Brunel University London. The chamber has a cut-off frequency of about 200 Hz. More detailed information about the anechoic chamber is given in [13]. A single $\frac{1}{2}$-inch G.R.A.S 46AE free-field microphone was installed at a distance of 1.4 m from the reference propeller in the plane of propeller rotation. A schematic view is shown in figure 1. The microphone's sensitivity is 50 mV/Pa and has an operating frequency range of 3.15 Hz to 20 kHz. A G.R.A.S 42AB sound calibrator is used to calibrate the microphone. An analog to a digital card from National Instruments is used to acquire the microphone signal. Data samples were collected for 20 sec at a sampling rate of 44 kHz, and they are windowed using a 2^{15} points fast Fourier transform with a 50 % overlap.

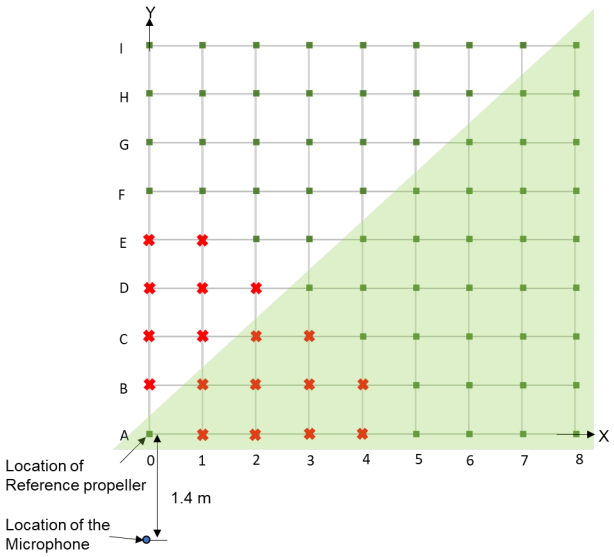

Fig. 1 Schematic showing 2D grid points for propeller movement and microphone location. Dimensions are not to scale.

The noise data in this work is presented in terms of Sound Pressure Level (SPL) and and Overall Sound Pressure level (OASPL). SPL is given by;

$$\text{SPL} = 20\log_{10}\left(\frac{P_{rms}}{P_{ref}}\right),\ \text{dB}$$

Here, P_{ref} is the reference pressure equals to 20 μPa and P_{rms} is the root mean square of the measured pressure fluctuations. The OASPL is calculated by integrating the acoustic pressure for (BPF-10 Hz) to (BPF+10 Hz) to capture the energy of the tonal peaks. Note that BPF is the Blade Pass Frequency. For the OASPL targeting the broadband noise region, the acoustic pressure is integrated between 5 and 10 kHz.

B. Test Stand

The in-house test rig and the photo of the anechoic chamber are shown in figure 2. The test rig is designed such that it gives a complete freedom of adjusting the positions of multiple propellers in various configurations. The rig is made with aluminium extrusion profiles that are covered by acoustic foams. Four vertical posts are attached on the base of the frame, out of which two posts were removed in the current campaign. These vertical posts can move along the *x* and*y* axis to provide different separation distances between propellers in the longitudinal and transverse directions, respectively. The frame was placed directly on the anechoic chamber floor and the whole mechanical structure is wrapped with acoustic foams to reduce the noise reflection from the metal surface. In order to minimise the aerodynamic disturbance during testing, all the cables were fastened on the backside of the posts.

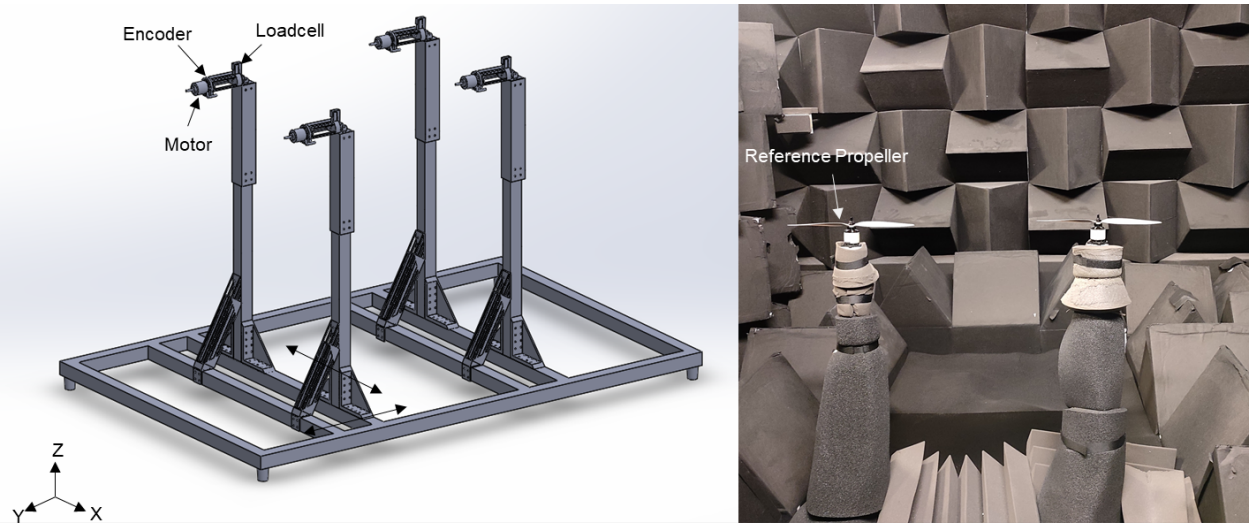

Fig. 2 Sketch of Test Stand (left), Photo of anechoic chamber showing reference and secondary propeller (right)

C. Test Setup

Experiments were conducted with APC 12x4.7 SF two-bladed propellers. The propellers are driven by the 880 KV electric brushless motor (T-Motor-AS 2820 Long Shaft) with a peak current of 45A. A 60A Emax BLHeli Series electronic speed controller (ESC) is incorporated to drive the motors. Each ESC draws power from an Outlander LiPo 4S 14.8V 3350 mAh 30C batteries to run the motors. A commercial software, RCbenchmark was used to control the speed of the motors. The motor is mounted on a 3D printed spacer which is connected to a single point load cell to assess the aerodynamic loads produced by the propeller. The data from the load cell is collected using a Phidget module (PhidgetBridge Wheatstone Bridge Sensor Interface). Rotational speed of the motor is measured using two optical encoders. The encoders have a resolution of 500 counts per revolution, and the data from encoder is acquired using Phidget Encoder board. It has an update rate of 125 sample per second, showing the exact motor rotational speed without any noticeable delay. The encoders and load cells were calibrated before capturing the results.

D. Test Variables

The experiments are performed on dual-propellers under the combination of the following influencing parameters, which are also summarised in table 1.

1 **Spatial Distributions in *x* and *y*:** The effect of separation distance is observed by nominating a reference propeller to be at a pre-fixed location, A0 [figure 1]. Note that the microphone depicted in figure 1 will always be

Description	RPM	Grid points	Result type
Reference propeller	3000, 3500, 4000	A0	Noise and Thrust
Single propeller	3500	A5-A8; B5-B8; G0-I0; G1-I1; H7-H8; I7-I8	Noise and Thrust
Dual propeller	3000, 3500, 4000	All grid locations	Noise and Thrust

Table 1 Test combinations

in the same plane as the reference propeller. The second propeller moves along the x and y axis throughout the grid, except at the points that are marked by red cross, so as to avoid physical interaction between propellers. The grid matrix is equal to 2D, where D is the diameter of the propeller, and each grid point is at D/4 distance apart in both x and y direction.

2 **RPM:** All the locations in the 2D grid described above were studied for 3000, 3500 and 4000 rotational speeds. .

3 **Number of Propellers:** Selective locations in the 2D grid were studied for Single and Dual propeller configurations to study the effect of interference. For the study of dual configuration, the propellers were not phase locked.

III. Preliminary Results

The following section discusses the aerodynamic and acoustics outcomes of the dual propellers highlighting the effect of interference with various separation distances. Although experiments were conducted for three different rotational speeds and at all the marked grid locations as mentioned above, results are shown only for 3500 rpm (unless mentioned otherwise) and at the locations between $0-45°$ azimuthal angle, highlighted by green color zone in figure 1. Aerodynamic and noise measurements were conducted simultaneously to compare the load fluctuation with the generated noise.

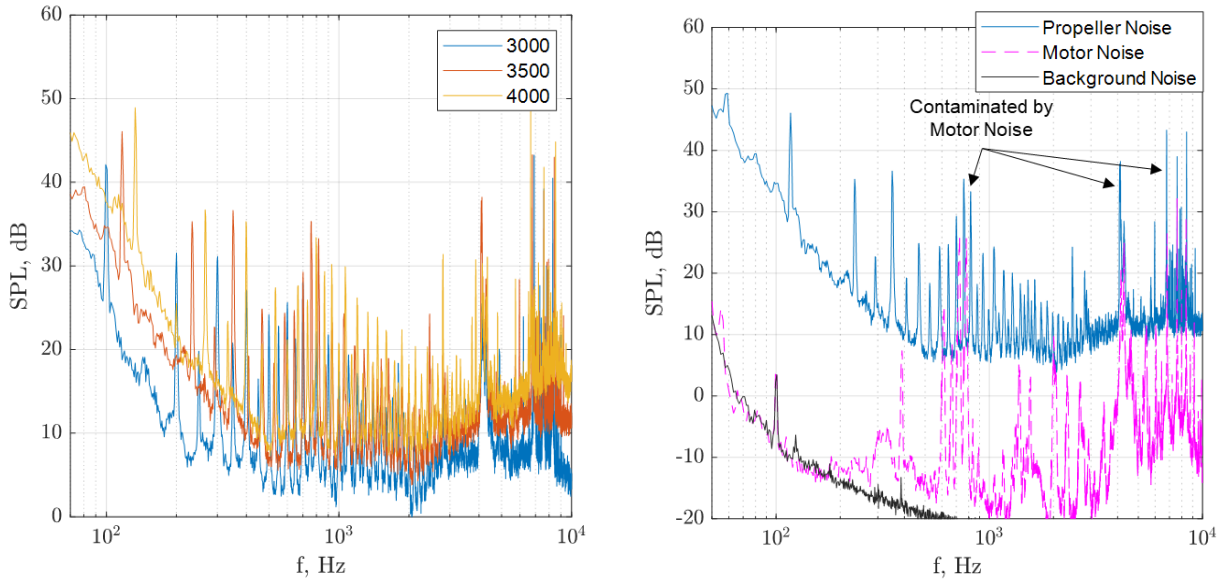

(a) **(b)**

Fig. 3 Comparison of SPL v/s frequency (a) at different RPMs (b) for Propeller noise at 3500 RPM, motor noise and background noise

A. Validation of the test rig

Prior to getting into the experiments with dual propellers and interference effect, the newly constructed rig is validated for varying rotational speeds. Sound Pressure Level with respect to the frequency plot for the reference propeller at three rotational speeds is shown in figure 3a.

Increasing the rotational speed shows increasing blade pass frequencies as well as the broadband noise level. These features are consistent with others, e.g. [2]. However, there are some tonal spikes present at the mid and high-frequency area. It is necessary to observe the contamination of the propeller spectrum with motor noise. Figure 3b shows the comparison between the propeller noise at 3500 rpm, motor noise and the ambient noise to highlight the possible frequency range of the propeller noise by the motor noise contamination. The results presented in this paper will bypass the frequency range where the motor noise is significant. Instead, the analysis will be primarily focused on the low-frequency noise, first three Blade Pass Frequencies (BPF) and mid to high-frequency broadband noise. The presence of motor noise in the acoustic spectra at small range of frequency is not expected to alter the conclusions made.

B. Effect of separation distance

1. Acoustic

In the present work, the separation distance between the propeller was varied by moving the second propeller through various grid points. This section presents the findings when the secondary propeller was moved away in transverse direction from grid location *A5* to *A8*. The SPL spectra were shown in figure 4, where the spectra for dual propellers at location *A5-A8* are compared against the reference propeller, which was run in the absence of a secondary propeller.

As was expected, the noise generation was increased for the case of dual propeller runs. The effect of the separation gap is clearly visible at low frequencies up to 400 Hz and at the harmonics of blade pass frequencies. While the gap is less than *2D*, the noise generation is the most significant when the separation distance between the propellers is the minimum, i.e. the *A5* case. The noise level then reduces as the distance increases up to *A7*. However, at *A8* where the gap is equal to *2D*, the noise generation trend is reversed where the spectrum closely follows the noise spectrum of the propeller at separation distance of *1.5D*, i.e. at the *A6*.

As the separation distance is reduced, the amplitude at the 1^{st} blade pass frequency is reduced where the lowest is at *A5*. For the entire range of separation distance between propellers (*A5-A8*), the mid to high frequency broadband noise remains almost consistent.

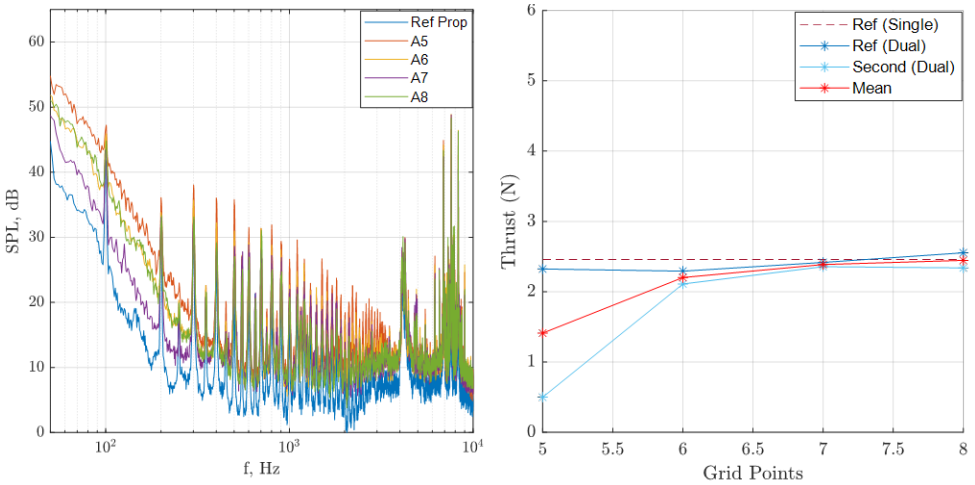

(a) 3000

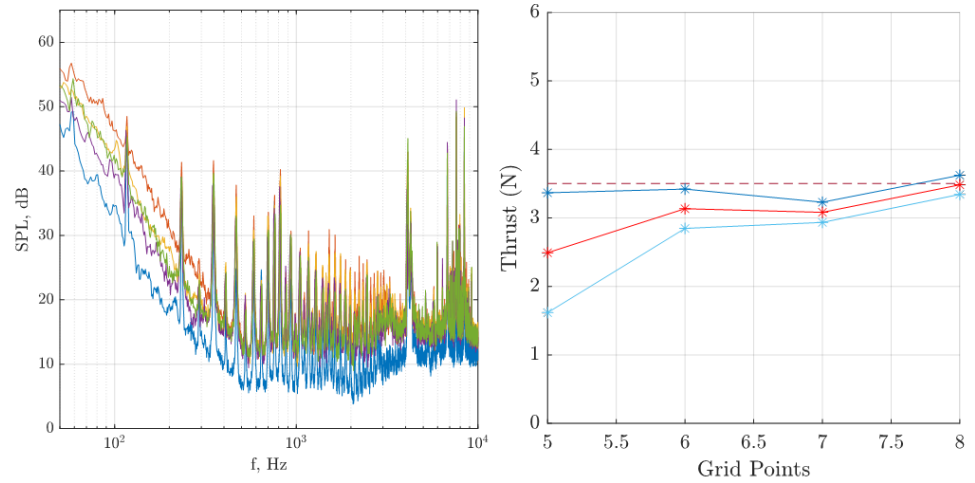

(b) 3500

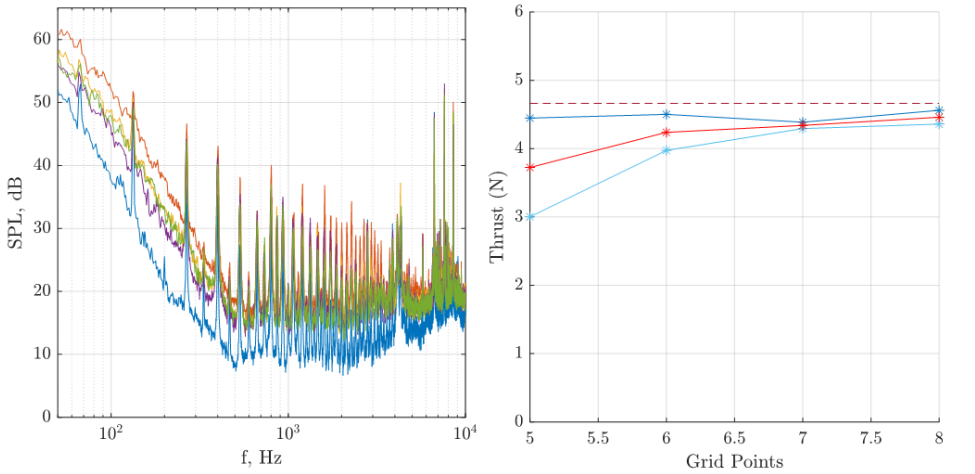

(c) 4000

Fig. 4 Comparison of Noise Spectra and respective mean thrust for dual propeller configuration at different locations compared with reference propeller

2. Aerodynamic

The aerodynamic comparison is evaluated for locations *A5-A8* (figure 4, right hand side) using averaged thrust data against the grid locations. The thrust plots show the reference propeller when runs independently as Ref (Single), the reference propeller and secondary propeller when run simultaneously in dual configuration as Ref (Dual) and Second (Dual), respectively, and the mean thrust of the two propellers in dual configuration as Mean. At all the rotational speeds a similar trend for the thrust at each grid location is observed. When the second propeller is closest to the reference propeller, which is at grid point *A5*, the mean thrust is lesser compared to the reference propeller. Recalling from the previous section, noise generation at this location is the maximum. When the separation gap is increased, the mean thrust slowly becomes closer to the thrust produced by the reference propeller. It is clear that the effect of separation distance can affect the thrust generation, which is highlighted by the fact that the thrust produced by the Ref (Dual) is lower than the Ref (Single). Ultimately, there is a close link between the aerodynamics forces and the noise generation for a multi-propeller system.

3. Propeller movement through 2D grid

To understand the overall effect of the propeller movement throughout the grid, contour maps (figure 5) were generated for the Overall Sound Pressure level (OASPL) corresponding to the narrowband components of 1^{st}, 2^{nd} and 3^{rd} BPF, as well as the broadband range of 5-10 kHz. The contour is shown only for $0-45°$ azimuthal angle and the x and y axes on the contour maps show the actual grid dimension in cm. The contour plots can be visualised as the effect generated by the second propeller, on the reference propeller in dual propeller configuration as observed from a fixed observation point. In the analysis thus far, there is no distance correction made, and these are the perceived noise at the microphone location when the second propeller is moved to various locations.

As the rotational speed increases for the 1^{st} BPF, the area affected by higher noise generation is increased. However, as the second propeller travels in both the transverse (x) and longitudinal (y) direction the tonal energy reduces, with an exception at 4000 rpm where there is again some region of high noise at large searation distance. This is similar to what was observed in the spectra presented earlier when the low frequency noise is louder when the two propellers are close and reduces as the secondary propeller moves away in the transverse direction. This effect becomes less significant at the 2^{nd} BPF, and even less so for the 3^{rd} BPF where the tones are only mildly affected by the distance. The high-frequency broadband noise does not show much affect when the propeller moves in the transverse direction, however as it moves down the grid in the y direction, there is a visible reduction.

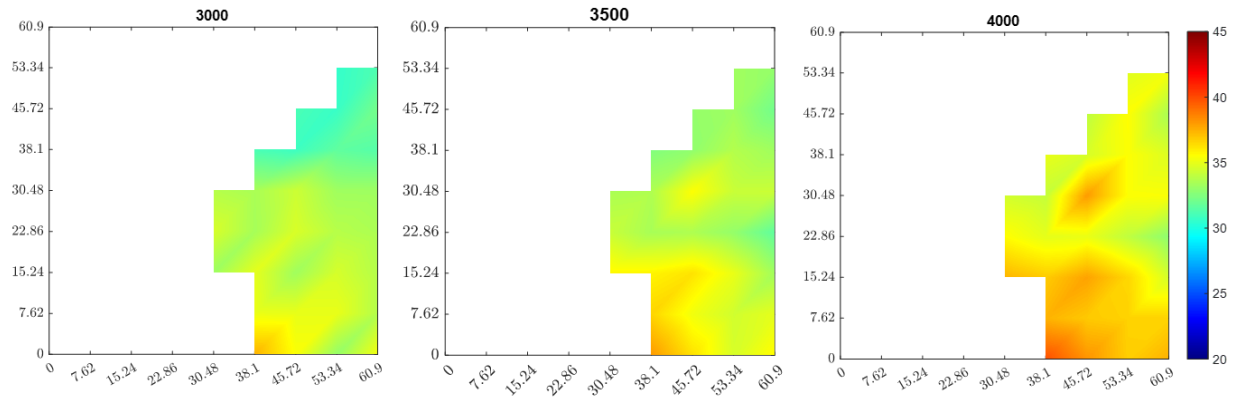

(a)

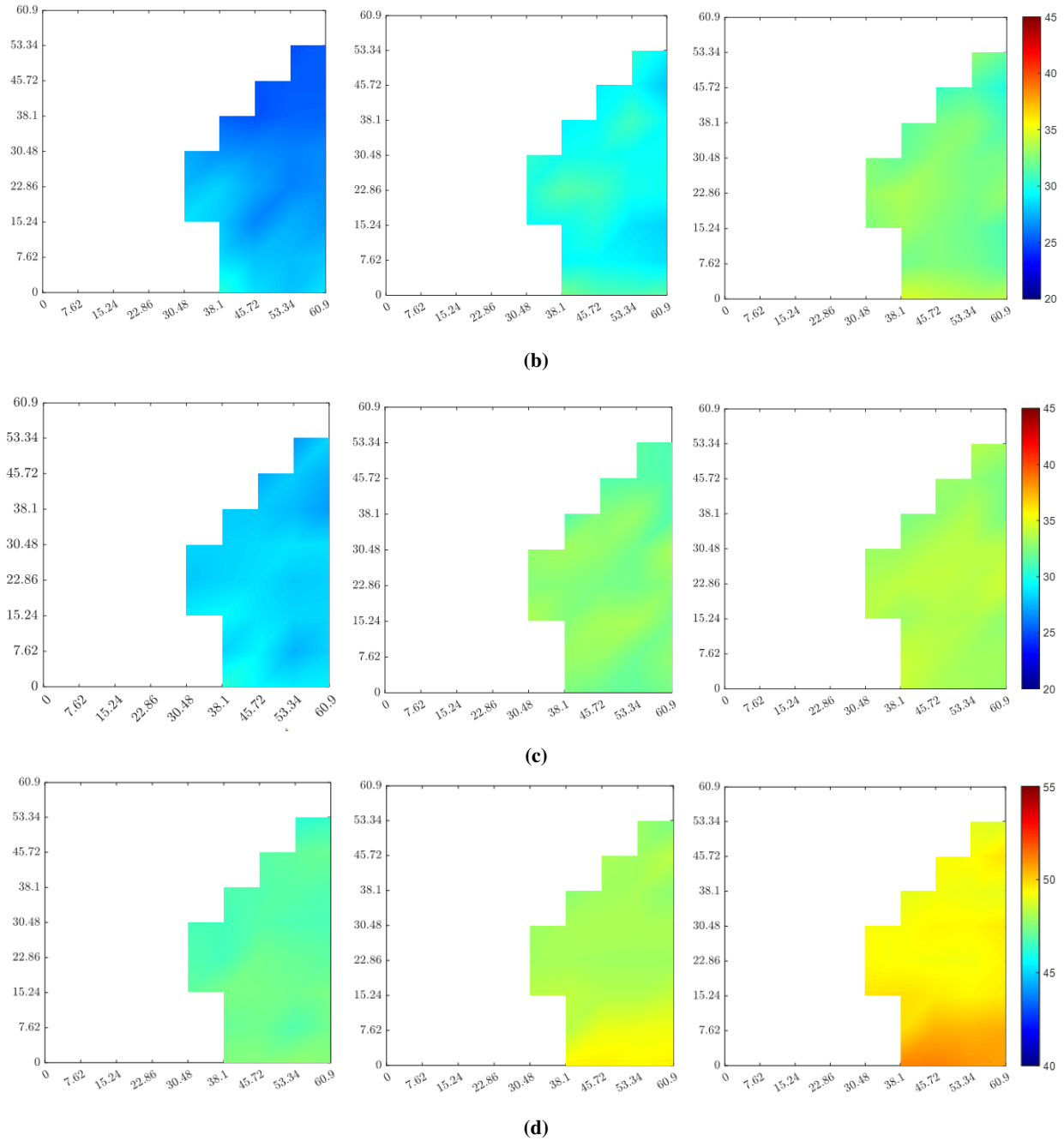

Fig. 5 OASPL for dual propeller configuration at 0-45 degree azimuthal location at (a) 1^{st} BPF, (b) 2^{nd} BPF, (c) 3^{rd} BPF and (d) High frequency broadband region between 5-10 kHz

C. Interference effect

1. Single propeller

In order to better understand the interference effect, first the noise performance of reference and secondary propellers were evaluated individually without the presence of another propeller. The sound pressure spectra for the secondary propellers at locations *A5-A8* (figure 6a) and *B5-B8* (figure 6b) are discussed here with reference propeller.

When the secondary propeller travels through different grid locations, broadband noise spectrum is almost unaffected.

But, there are slight variations observed in the tonal component. The reference propeller, being in line with the microphone, shows higher noise at low frequency region, which was even observed at other rotational speeds in former section. The broadband component on the other hand gets lower than that at the other locations between 400 Hz to 3000 Hz after which it merges with the other spectrums. There is some disruption observed at *B8* location at low frequencies.

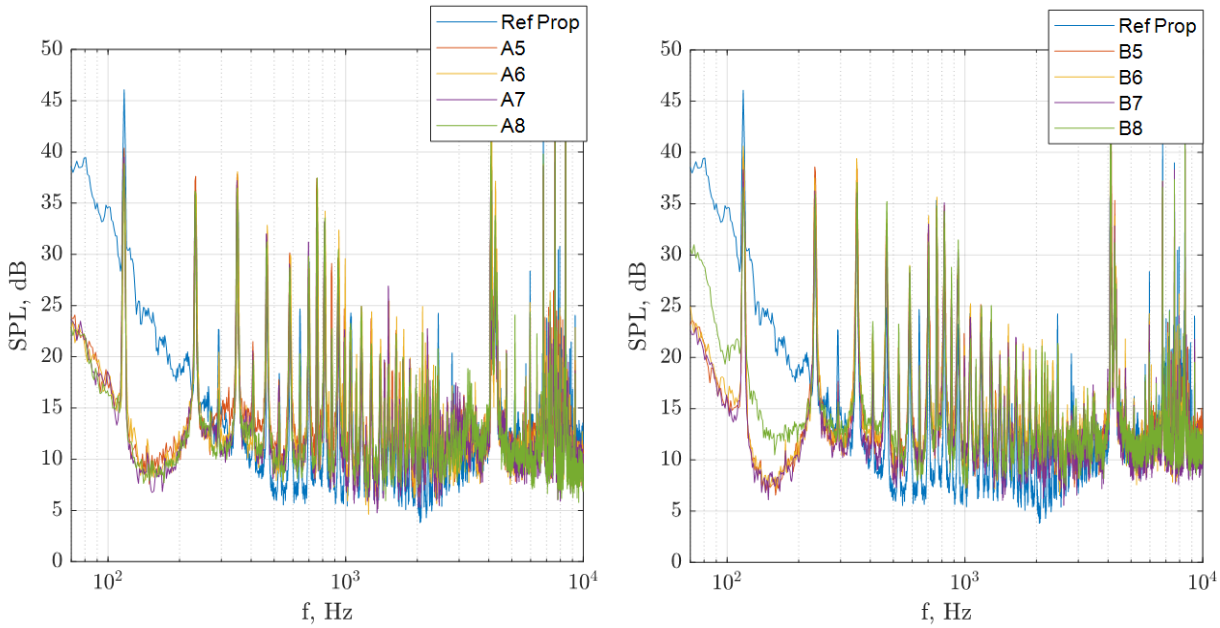

(a) **(b)**

Fig. 6 Noise spectrum for single propeller compared with reference propeller at location (a)A5-A8 (b)B5-B8

2. Dual and combined spectrum

After obtaining the individual spectrums of single propeller, the two spectra from individual propellers (Reference and secondary) are added, similar to the method followed in [7]. The combined spectrum (Ref Prop + Single) is compared with the spectrum of dual propellers (Dual)for the grid locations *A5-A8* in figure 7. Individual spectrums (Ref Prop and Single) are shown for the reference. The addition of the two spectrums are done for the acoustic pressures, before obtaining the sound pressure level to avoid the amplification of tones. It is also to be noted that, there is no distance correction done, to keep the single propeller spectrum results consistent with dual propeller spectrum.

When the two single spectrums are combined, the broadband noise below 350 Hz is approximately 5-10 dB lower compared to dual spectrum, but is noticed to follow the combined spectrum in mid frequency range. The tones are higher for the combined spectrum for first 9 fundamental frequencies except at 4^{th} and 8^{th} BPF, which could be due to contamination with motor noise, from 10^{th} BPF onwards the tones for dual spectrum show dominance. Multiples of half BPF are steadily higher for the combined spectrum. As the propeller moved further apart from *A5* to *A7*, the low frequency broadband noise is reduced, which again increases at *A8* location. Broadband oscillation between mid to high frequency diminishes. Tonal components at *A6* follow the same trend as the location *A5*, however when increasing the distance to *A7* and *A8*, the combined propeller shows higher tones compared with dual spectrum.

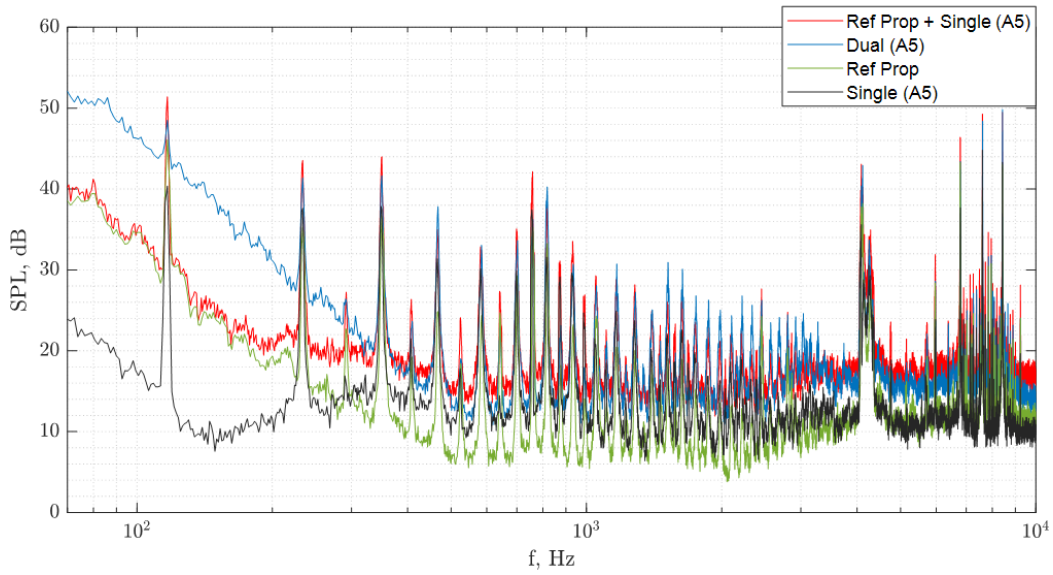
Ref Prop + Single (A5)
Dual (A5)
Ref Prop
Single (A5)
SPL, dB
f, Hz

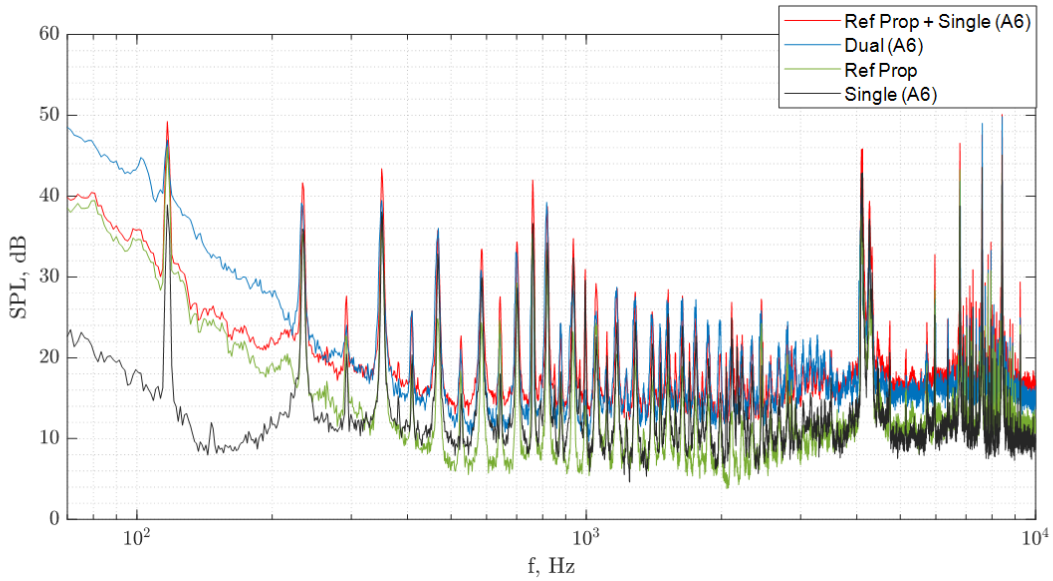
Ref Prop + Single (A6)
Dual (A6)
Ref Prop
Single (A6)
SPL, dB
f, Hz

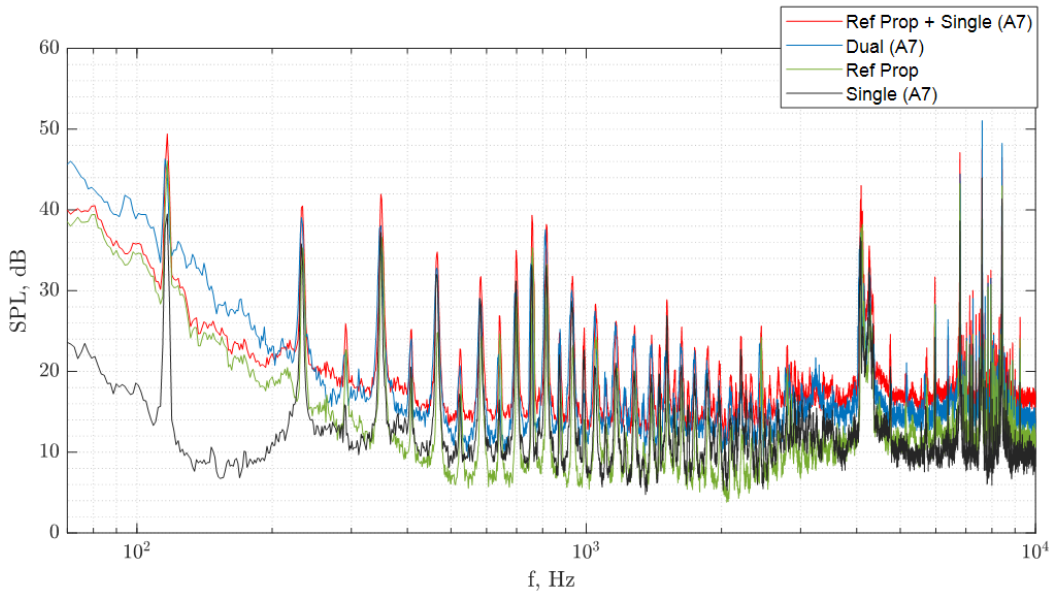
Ref Prop + Single (A7)
Dual (A7)
Ref Prop
Single (A7)
SPL, dB
f, Hz

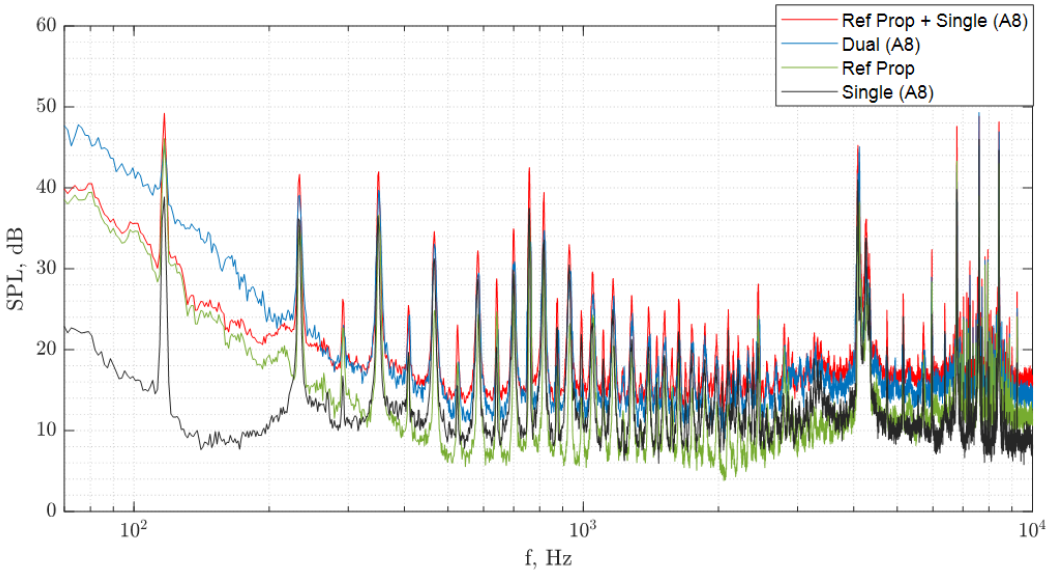

Fig. 7 Comparison of combined spectrum with dual propeller spectrum at location *A5, A6, A7, A8*

Similar observations were made at locations *H7, H8* and *I8* (figure 8), where the two propellers are at the farthest points in the grid. The spectrum here displays a better picture of the presence of interference effect when the second propeller in dual propeller configuration advances down the grid, dual propeller spectrum becomes slightly lower than the combined spectrum and follows the broadband component. At Location *I8*, due to strong interference, the spectrum at low frequency is reduced well below the superimposed spectrum, and oscillates slightly around the combined spectrum in mid to high frequency region. The tones do not follow a pattern here and have some fluctuations.

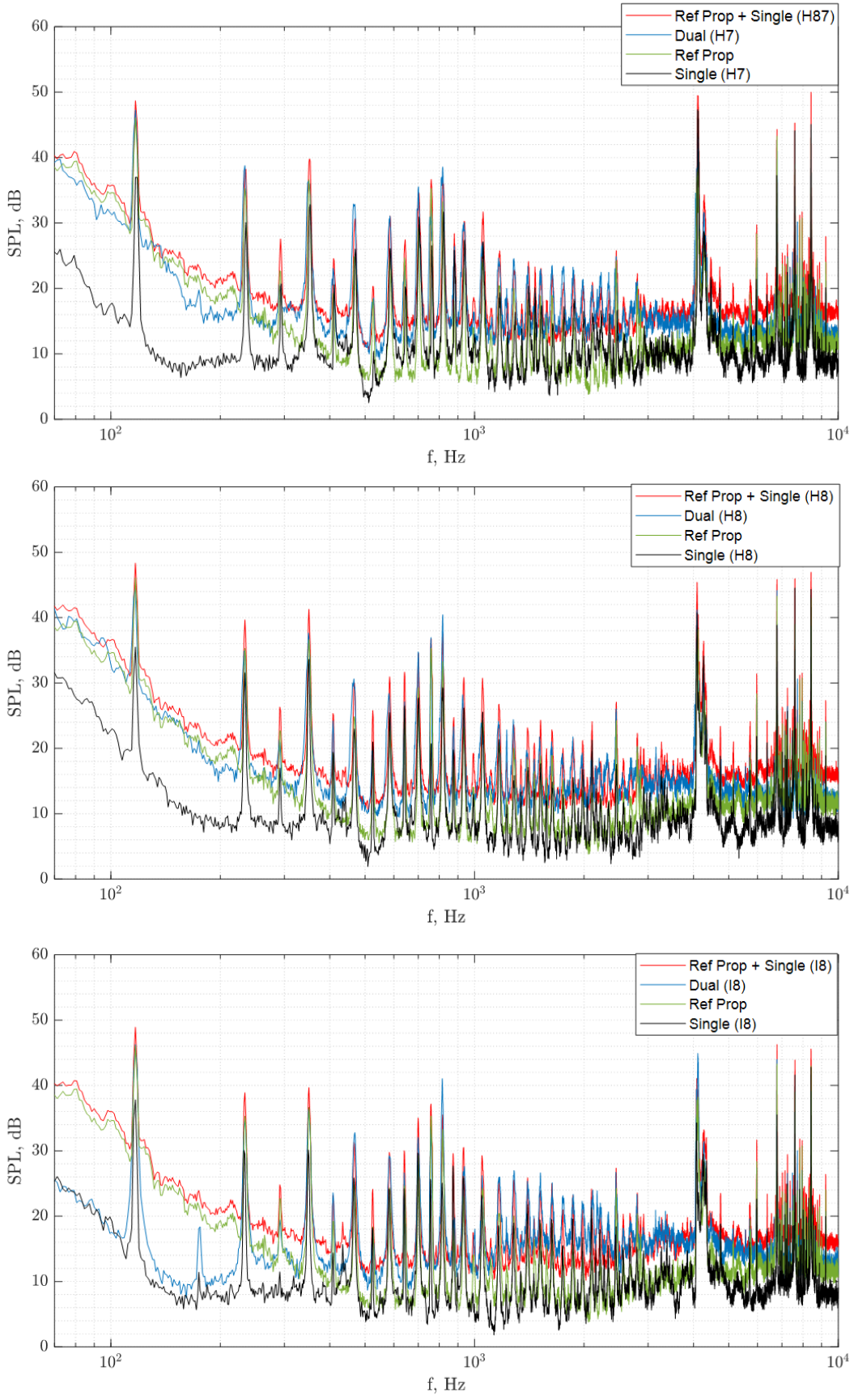

Fig. 8 Comparison of combined spectrum with dual propeller spectrum at location *H7*, *H8* and *I8*

IV. Conclusion

This paper presents some preliminary results of the experiments performed on a multi-propeller configuration. Based upon the results presented so far, the mean aerodynamic loading is affected when the two propellers are in close proximity, but becomes almost similar to the reference as the distance increases.

The complex behaviours of acoustics interactions are predominant at low frequencies for the separation in the transverse (side-by-side) direction with respect to the microphone location, but the mid to high frequency broadband spectrum is only mildly affected. When the secondary propeller moves along the longitudinal (tandem) eccentricity, the tones for the first BPF and high frequency broadband noise show a considerable reduction in the overall sound pressure level. The second and third BPF frequencies, however, show a minimal variation.

To determine the dominance of the interference effect for a two propeller configuration, one could add the two individual spectrum pertaining to single propeller at the respective locations, and compare it against the measured spectrum of the multi-propeller operated simultaneously. It is found that the comparison is dictated by the location of the two propellers.

Although the results are indicative of a strong interference effect between the propellers, a more complete picture for a wider range of configurations, as well as the physics behind it will only be deduced after further experimentation.

References

[1] Cervatius, M., "Can air taxis become a democratic and sustainable means of transportation?" , 2021. URL `Canairtaxisbecomeademocraticandsustainablemeansoftransportation_.html`.

[2] Jordan, W. A., Narsipur, S., and Deters, R., "Aerodynamic and Aeroacoustic Performance of Small UAV Propellers in Static Conditions," *AIAA AVIATION 2020 FORUM*, 2020, p. 2595. https://doi.org/10.2514/6.2020-2595.

[3] Jamaluddin, N. S., Celik, A., Baskaran, K., Rezgui, D., and Azarpeyvand, M., "Aeroacoustic performance of propellers in turbulent flow," *AIAA Aviation 2021 Forum*, 2021, p. 2188.

[4] Brungart, T. A., Olson, S. T., Kline, B. L., and Yoas, Z. W., "The reduction of quadcopter propeller noise," *Noise Control Engineering Journal*, Vol. 67, No. 4, 2019, pp. 252–269.

[5] Zhou, W., Ning, Z., Li, H., and Hu, H., "An experimental investigation on rotor-to-rotor interactions of small UAV propellers," *35th AIAA applied aerodynamics conference*, 2017, p. 3744. https://doi.org/10.2514/6.2017-3744.

[6] Bu, H., Ma, Z., and Zhong, S., "An experimental investigation of noise characteristics of overlapping propellers," *The Journal of the Acoustical Society of America*, Vol. 152, No. 1, 2022, pp. 591–600. https://doi.org/10.1121/10.0012735.

[7] Bu, H., Wu, H., Bertin, C., Fang, Y., and Zhong, S., "Aerodynamic and acoustic measurements of dual small-scale propellers," *Journal of Sound and Vibration*, Vol. 511, 2021, p. 116330. https://doi.org/10.1016/j.jsv.2021.116330.

[8] de Vries, R., van Arnhem, N., Sinnige, T., Vos, R., and Veldhuis, L. L., "Aerodynamic interaction between propellers of a distributed-propulsion system in forward flight," *Aerospace Science and Technology*, Vol. 118, 2021, p. 107009. https://doi.org/10.1016/j.ast.2021.107009.

[9] Zanotti, A., and Algarotti, D., "Aerodynamic interaction between tandem overlapping propellers in eVTOL airplane mode flight condition," *Aerospace Science and Technology*, Vol. 124, 2022, p. 107518. https://doi.org/10.1016/j.ast.2022.107518.

[10] Celik, A., Jamaluddin, N. S., Baskaran, K., Rezgui, D., and Azarpeyvand, M., "Aeroacoustic Performance of Rotors in Tandem Configuration," *AIAA AVIATION 2021 FORUM*, 2021, p. 2282. https://doi.org/10.2514/6.2021-2282.

[11] Shukla, D., Hiremath, N., and Komerath, N. M., "Low Reynolds number aerodynamics study on coaxial and quad-rotor," *2018 Applied Aerodynamics Conference*, 2018, p. 4118. https://doi.org/10.2514/6.2018-4118.

[12] Paruchuri, C. C., Joseph, P., Akiwate, D. C., Parry, A. B., and Prior, S. D., "On the noise generation mechanisms of overlapping propellers," *AIAA AVIATION 2021 FORUM*, 2021, p. 2281. https://doi.org/10.2514/6.2021-2281.

[13] Vathylakis, A., Chong, T. P., and Kim, J. H., "Design of a low-noise aeroacoustic wind tunnel facility at Brunel University," *20th AIAA/CEAS Aeroacoustics Conference*, 2014, p. 3288. https://doi.org/10.2514/6.2014-3288.